ELSEVIER

Application of a nonlinear stress–strain model to axisymmetric turbulent swirling flows

K. M. Wall and D. B. Taulbee
Department of Mechanical and Aerospace Engineering, Jarvis Hall, State University of New York at Buffalo, Amherst, New York, USA

A nonlinear stress–strain relation (NLSM) for the turbulence stresses is applied to axisymmetric free shear flows with and without swirl. This relation is an explicit solution to an algebraic Reynolds stress model (ARSM). The stress relation is a finite sum of tensor groups depicting various interactions between the mean strain and vorticity fields. Implementation is in the context of a $k-\epsilon$ type model. Comparisons are made between flow field predictions obtained with the full Reynolds stress model, the NLSM corresponding to improved and standard ARSMs, the $k-\epsilon$ model and experimental data.

Keywords: stress relation; turbulence modeling; axisymmetric flows

Introduction

The idea of formulating the algebraic Reynolds stress model (ARSM) from the Reynolds stress transport equations originated with Launder (1971) and Rodi (1972). These formulations consist of approximating the convection and diffusion terms in some fashion so that the modeled differential equations for the Reynolds stress tensor becomes algebraic. Rodi (1976) postulated that the convection minus diffusion terms in the dynamic equation for the Reynolds stress be proportioned to the convection minus diffusion terms in the turbulent kinetic energy equation. The resulting expression for the ARSM is $\overline{(u_i u_j}/k)(P-\epsilon) = P_{ij} + \Phi_{ij} - \epsilon_{ij}$. The Reynolds stresses can then be obtained for some model of the pressure strain Φ_{ij} and the dissipation tensor approximated by $\epsilon_{ij} = 2\epsilon\delta_{ij}/3$, for large turbulence Reynolds numbers. This is the basic formulation for most ARSMs in use today.

The ARSM has been applied to a wide variety of near parallel flow situations and has been successful in accounting for the effects of longitudinal surface curvature, rotation, buoyancy, etc. The $k-\epsilon$ model has been employed successfully to strong swirling flows (see, for example, Leschziner and Rodi (1984) and Naji (1986)), but only with the use of ad hoc swirl-dependent modifications. Kim and Chung (1988) concluded that the ARSM was more capable of predicting the strong swirling jet with recirculation than the $k-\epsilon$ model. The ARSM has inherent deficiencies. Fu et al. (1988), utilizing the ARSM and the full Reynolds stress model (RSM) in the axisymmetric jet with and without swirl, attributed errors in predictions with the ARSM to the approximations of the convective and diffusive processes in its formulation.

It is generally thought that the ARSM is valid for near equilibrium flows where convection and diffusion assume a certain balance. Taulbee (1992) showed that the standard ARSM is valid only in the asymptotic limit where the anisotropic stress tensor becomes constant. This requires a large value of a time-scales parameter $\tau\sigma$ defined as the ratio of the time scale of the turbulence $\tau = k/\epsilon$ to that of the mean flow strain field $1/\sigma$ where $\sigma = (S_{kl}S_{lk})^{1/2}$. Taulbee (1992) formulated an improved ARSM that approximately represents the particular solution of the modeled Reynolds stress equation (with transport neglected) over the complete range of the time-scales parameter. Hence, the improved ARSM will more closely duplicate the behavior of the differential Reynolds stress equation.

When the ARSM is employed in general two- or three-dimensional (2-D or 3-D) flows a system of algebraic equations needs to be solved for the stresses. Usually the solution to the equation set is carried out numerically at each time step or iteration in the overall numerical procedure. Because there is no diffusion or damping in the equation set, it is very difficult to maintain a stable numerical solution. Hence, it is desirable to employ an explicit stress–velocity field relation, and thus provide stability to the numerical procedure. Taulbee et al. (1994) formulated a nonlinear stress–strain relation (NLSM) for 3-D flows that is an explicit closed-form solution to the ARSM equation set. The NLSM contains a finite sum of tensor groups involving the mean strain and vorticity fields.

In this paper, we examine predicted results for axisymmetric shear flows utilizing the RSM, the $k-\epsilon$ model, and the NLSM for the standard and improved ARSMs. Also, for the axisymmetric swirling jet, results are obtained using the improved ARSM/NLSM with convective terms from a curvilinear coordinate system. Results with the improved ARSM/NLSM compared favorably to results with the full RSM.

Address reprint requests to Prof. D. B. Taulbee, Dept. of Mechanical and Aerospace Engineering, University of Buffalo, Jarvis Hall, Amherst, NY 14260, USA.

Received 14 March 1995; accepted 2 October 1995

Int. J. Heat and Fluid Flow 17: 116–123, 1996

655 Avenue of the Americas, New York, NY 10010

0142-727X/96/$15.00
SSDI 0142-727X(95)00084-4

Model formulation

From the modeled transport equations for the Reynolds stress, Taulbee (1992) derived the ARSM in the form

$$a = -\tfrac{8}{15}S - C_3\left[aS + Sa - \tfrac{2}{3}\{aS\}I\right] + C_4(a\Omega - \Omega a) \qquad (1)$$

where a is the matrix of the anisotropic stress components, $a_{ij} = \overline{u_i u_j}/k - 2\delta_{ij}/3$; S is the matrix of the nondimensional mean flow strain components, $S^*_{ij} = g\tau(\partial U_i/\partial x_j + \partial U_j/\partial x_i)/2$; Ω is the matrix of the nondimensional mean flow rotation components, $\Omega^*_{ij} = g\tau(\partial U_i/\partial x_j - \partial U_j/\partial x_i)/2$; $\tau = k/\epsilon$ is the time scale of the turbulence; I is the identity matrix; and $\{aS\}$ is the trace of aS. The variable g in the definitions of S and Ω is given by:

$$g = \left(C_1 - 1 + \frac{P}{\epsilon}\right)^{-1} \qquad (2)$$

for the standard ARSM as given by Rodi (1976), and

$$g = \left[C_1 + C_{\epsilon_2} - 2 + \left(2 - C_{\epsilon_1}\right)\frac{P}{\epsilon}\right]^{-1} \qquad (3)$$

for the improved ARSM as given by Taulbee (1992). This formulation is designed to match the behavior of the RSM at small turbulence time scales as well as at large values that correspond to the standard ARSM. The parameters C_3 and C_4 appear in the rapid part of the pressure-strain correlation

$$\Phi_{ij} = -C_1\epsilon a_{ij} + C_0 k S_{ij} + (1 - C_3) \times k\left(a_{il}S_{lj} + a_{jl}S_{li} - \tfrac{2}{3}a_{lm}S_{ml}\delta_{ij}\right) - (1 - C_4)k\left(a_{il}\Omega_{lj} + a_{jl}\Omega_{li}\right) \qquad (4)$$

which is linear in a_{ij}. The pressure-strain correlation defined by Equation 4 is equivalent to that given by Launder et al. (1975) and the parameters C_0, C_3, and C_4 can be written in terms of a single parameter C_2. Taulbee et al. (1994) analyzed homogeneous shear flow experiments and give $C_2 = 0.52$, which results in the values $C_0 = 0.8$, $C_3 = 0.029$, and $C_4 = 0.422$. The parameter C_1 appears in the slow part of Equation 4, and C_{ϵ_1} and C_{ϵ_2} appear in the modeled equation for the dissipation. For this work, we use values of $C_1 = 1.8$, $C_{\epsilon_1} = 1.44$, and $C_{\epsilon_2} = 1.92$.

Ekander and Johansson (1989), examining curved and rotating channel flows, concluded that the extra convection terms resulting from a transformation to a curvilinear coordinate system are redistributive and should be included in the formulation of the ARSM. These convection terms arising from coordinate curvature can be included in the ARSM by defining the matrix of the mean flow rotation tensor as follows:

$$\Omega = \Omega^*_{ij} = g\tau\left[\Omega^i_j + \left\{\begin{matrix} i \\ jm \end{matrix}\right\}\frac{U^m}{C_4}\right] \qquad (5)$$

for use in Equation 1. In this equation the curly-bracket term is the Christoffel symbol of the second kind. As seen later, this formulation is essential for obtaining the proper behavior for certain stress components.

A nonlinear stress–strain relation (NLSM) for 3-D flows was obtained by Taulbee et al. (1994) via a closed-form solution of the linear algebraic equation set given by Equation 1. The resulting solution has the following form:

$$a = \sum_{n=1}^{10} G^{(n)}T^{(n)} \qquad (6)$$

where the $T^{(n)}$ are independent symmetric traceless tensor groups in S and Ω:

$$\begin{aligned} T^{(1)} &= S & T^{(6)} &= \Omega^2 S + S\Omega^2 - \tfrac{2}{3}I_4 I \\ T^{(2)} &= S\Omega - \Omega S & T^{(7)} &= \Omega S\Omega^2 - \Omega^2 S\Omega \\ T^{(3)} &= S^2 - \tfrac{1}{3}I_1 I & T^{(8)} &= S\Omega S^2 - S^2\Omega S \\ T^{(4)} &= \Omega^2 - \tfrac{1}{3}I_2 I & T^{(9)} &= \Omega^2 S^2 + S^2\Omega^2 - \tfrac{2}{3}I_5 I \\ T^{(5)} &= \Omega S^2 - S^2\Omega & T^{(10)} &= \Omega S^2\Omega^2 - \Omega^2 S^2\Omega \end{aligned} \qquad (7)$$

where $I_1 = \{S^2\}$, $I_2 = \{\Omega^2\}$, $I_3 = \{S^3\}$, $I_4 = \{S\Omega^2\}$ and $I_5 =$

Notation

a_{ij}	anisotropic stress tensor, $\overline{u_i u_j}/k - 2\delta_{ij}/3$
C_1	linear return-to-isotropy coefficient
C_2	linear rapid coefficient
C_3	linear rapid coefficient, $(5 - 9C_2)/11$
C_4	linear rapid coefficient, $(1 + 7C_2)/11$
C_ϵ	dissipation transport coefficient
C_{ϵ_1}, C_{ϵ_2}	dissipation equation coefficients
C_μ	eddy-viscosity constant in $k - \epsilon$ model
C_s	stress transport coefficient
I	indentity matrix
k	turbulent kinetic energy, $\overline{u_i u_i}/2$
$\overline{P}$	pressure
P	production rate of turbulent kinetic energy, $P_{ii}/2$
P_{ij}	generation rate of Reynolds stress tensor, $-(\overline{u_i u_l}\partial U_j/\partial x_l + \overline{u_j u_l}\partial U_i/\partial x_l)$
S	matrix of the nondimensional mean flow strain components, $S^*_{ij} = g\tau S_{ij}$
S_{ij}	mean flow strain tensor, $(\partial U_i/\partial x_j + \partial U_j/\partial x_i)/2$
T_{ijl}	transport of Reynolds stress, $C_s(k/\epsilon)\overline{u_i u_m}\partial\overline{u_i u_j}/\partial x_m$
U_i, u_i	x_i component of the mean and fluctuating velocities
$\overline{u_i u_j}$	Reynolds stress tensor
U, u	mean and fluctuating velocities in (axial) x-direction
V, v	mean and fluctuating velocities in (radial) r-direction
W, w	mean and fluctuating velocities in (angular) θ-direction

Greek

γ	linear rapid coefficient, $4(15C_2 - 1)/55$
δ_{ij}	Kroneker delta
ϵ	dissipation rate of k
ϵ_{ij}	dissipation rate tensor, $2\epsilon\delta_{ij}/3$
ν_t	turbulence viscosity coefficient
τ	turbulence time-scale, k/ϵ
Ω	matrix of the nondimensional mean flow vorticity components, $\Omega^*_{ij} = g\tau\Omega_{ij}$
Ωij	mean flow vorticity tensor, $(\partial U_i/\partial x_j - \partial U_j/\partial x_i)/2$

$\{S^2\Omega^2\}$ are independent invariants and $\{\}$ denotes the trace; i.e., $\{S^2\} = S^*_{kl}S^*_{lk}$. The $G^{(n)}$ take the form

$$G^{(1)} = -\frac{8}{15D}(2 - 7C_4^2I_2) + C_3\frac{64}{15D^2}C_4^2I_4(1 - 7C_4^2I_2 + C_4^4I_2^2)$$

$$G^{(2)} = -\frac{16}{15D}C_4(1 - 2C_4^2I_2) + C_3\frac{32}{15D^2}C_4^3I_4(5 - C_4^2I_2)(1 - 2C_4^2I_2)$$

$$G^{(3)} = C_3\frac{32}{15D}(1 - 2C_4^2I_2)$$

$$G^{(4)} = -\frac{32}{5D}C_4^4I_4 - C_3\frac{16}{5D}c_4^2\left[I_1 - \frac{4}{D}C_4^2(7 - 2C_4^2I_2)I_4\right]$$

$$G^{(5)} = -C_3\frac{16}{5D}C_4$$

$$G^{(6)} = -\frac{16}{5D}C_4^2 + C_3\frac{32}{5D^2}C_4^4I_4(7 - 2C_4^2I_2)$$

$$G^{(7)} = \frac{16}{5D}C_4^3 - C_3\frac{32}{5D^2}C_4^5I_4(7 - 2C_4^2I_2)$$

$$G^{(8)} = 0$$

$$G^{(9)} = C_3\frac{32}{5D}C_4^2$$

$$G^{(10)} = 0 \qquad (8)$$

where $D = (1 - 2C_4^2I_2)(2 - C_4^2I_2)$. Equation 6, with $T^{(n)}$ and $G^{(n)}$ given by Equations 7 and 8, represents an explicit relation for the anisotropic Reynolds stress tensor in terms of the mean flow velocity field. It should be pointed out that this solution to Equation 1 requires that the model parameter C_3 be relatively small (see Taulbee et al. 1994), $C_3 = 0.029$ in this work. The stresses given by Equation 6 are utilized in a $k - \epsilon$ type model.

Application to axisymmetric flows

Flow field predictions were obtained for axisymmetric free shear flows with and without swirl. If the normal strains $(\partial U/\partial x,\ \partial V/\partial r,\ V/r)$ are retained for the axisymmetric jet without swirl, a 3-D stress relation should be used. If the normal strains are neglected, leaving only the shear strain $S_{xr} = (\partial U/\partial r)/2$, then the 2-D stress relation given in Taulbee (1992) can be used. A 3-D stress relation must be used in calculations of the axisymmetric swirling jet, because at a minimum the S_{xr} and $S_{\theta r} = (\partial W/\partial r - W/r)/2$ components must be retained. The normal strains are consistently retained here, Launder and Morse (1979) have shown that their effect can be somewhat significant. Also, it is known that there are elliptic effects that can somewhat affect the results. However, we are primarily interested in comparisons between models, so the simpler parabolic formulation and stream-wise marching numerical solution have been used. Besides, as is well known, a $k - \epsilon$ model, ARSM or RSM that predicts 2-D flows well, will not accurately predict axisymmetric flows unless some modification is made to the model, in particular, to the dissipation equation.

The equations of motion and the model equations for k and ϵ, for axisymmetric flows, come from Rodi and Leschziner (1984). The fluid density ρ being constant has been absorbed into the variable for the pressure P. These equations are given below.

Conservation of mass:

$$\frac{\partial U}{\partial x} + \frac{1}{r}\frac{\partial(rV)}{\partial r} = 0 \qquad (9)$$

Conservation of axial momentum:

$$\frac{\partial(UU)}{\partial x} + \frac{1}{r}\frac{\partial(rUV)}{\partial r} = -\frac{\partial \bar{P}}{\partial x} - \frac{1}{r}\frac{\partial(r\overline{uv})}{\partial r} \qquad (10)$$

Conservation of radial momentum:

$$\frac{\partial \bar{P}}{\partial r} = \frac{W^2}{r} \qquad (11)$$

Conservation of angular momentum:

$$\frac{\partial(UW)}{\partial x} + \frac{1}{r}\frac{\partial(rVW)}{\partial r} + V\frac{W}{r} = -\frac{1}{r}\frac{\partial(r\overline{vw})}{\partial r} - \frac{\overline{vw}}{r} \qquad (12)$$

Turbulence kinetic energy:

$$\frac{\partial(kU)}{\partial x} + \frac{1}{r}\frac{\partial(rkV)}{\partial r} = \frac{1}{r}\frac{\partial}{\partial r}\left[rC_s\frac{k}{\epsilon}\overline{v^2}\frac{\partial k}{\partial r}\right] + P - \epsilon \qquad (13)$$

Turbulence dissipation:

$$\frac{\partial(\epsilon U)}{\partial x} + \frac{1}{r}\frac{\partial(r\epsilon V)}{\partial r} = \frac{1}{r}\frac{\partial}{\partial r}\left[rC_\epsilon\frac{k}{\epsilon}\overline{v^2}\frac{\partial \epsilon}{\partial r}\right] + (C_{\epsilon_1}P - C_{\epsilon_2}\epsilon)\frac{\epsilon}{k} \qquad (14)$$

For the axisymmetric jet without swirl, Equations 11 and 12 are not required, and $\partial P/\partial x$ is neglected in Equation 10. The equations for k and ϵ include the diffusion closures used in full Reynolds stress modeling. These formulations are used in the calculations with the ARSM, as well as with the RSM, because the derivation of the ARSM is in the context of Reynolds stress modeling. For calculations with the $k - \epsilon$ model the coefficient $C_\mu(k^2/\epsilon)$ replaces $C_s(k/\epsilon)\overline{v^2}$ in Equations 13 and $C_\mu(k^2/\epsilon)/\sigma_\epsilon$ replaces $C_\epsilon(k/\epsilon)\overline{v^2}$ in Equation 14, where $C_\mu = 0.09$ and $\sigma_\epsilon = 1.3$. Standard values are used for the parameters $C_s = 0.22$ and $C_\epsilon = 0.18$, as given by Launder et al. (1975).

The turbulence stresses were calculated from application of the NLSM of Equation 6, the full RSM, and the $k - \epsilon$ model. Results obtained with the NLSM and g defined by Equation 2 or 3 are referred to as standard or improved ARSM results, respectively. The RSM equations, as given by Launder and Morse (1979), written for the axisymmetric swirling jet are given in Appendix A. These contain the same pressure-strain correlation as in Equation 4. The strain and vorticity tensor components are listed in Appendix B. For the axisymmetric jet without swirl, the RSM equations and the strain and vorticity tensor components are given by setting $W = 0$ in the definitions in Appendices A and B. Calculations were also made with an NLSM with Ω defined by Equation 5 and g from Equation 3. This is the same as the improved ARSM but with corrections to account for a curvilinear coordinate system. The components of the vorticity tensor Ω defined in Equation 5 are listed in Appendix C for the axisymmetric swirling jet. It should be noted that there are no extra terms in the definition of Ω for the axisymmetric jet without swirl.

Results and discussion

Previous works by Gibson and Younis (1986), Fu et al. (1988), Hogg and Leschziner (1989), and Jones and Pascau (1989) have established that the RSM is better than the $k - \epsilon$ model at reproducing the major features of swirling flows. Gibson and Younis found the RSM to be adequate at reproducing experimental results for weak swirling flows. Hogg and Leschziner and Jones and Pascau applied the RSM and $k - \epsilon$ model to strong swirling confined flows and concluded that the RSM has the proper mechanism to account for swirl dependent effects. Al-

though predictions of the swirling jet are plotted along with experimental data in this paper, comparison to experimental data is not the main interest here. Because the goal of this work is to obtain results with the same quality as those from the RSM, emphasis is placed on comparisons with RSM results.

There has been much discussion in the literature concerning comparison of turbulence model predictions to experimental data (see Taulbee 1989). Usually, differences between measured data and predictions are blamed on the inadequacy of the turbulence model. However, for some flows the quality of the available experimental data is questionable. Recently, Hussein et al. (1994) have shown that, for the axisymmetric jet, the turbulence intensity levels and experimental environment can significantly affect the measured data. They concluded that turbulence levels that are greater than 10% of the mean flow will cause significant errors in the experimental data when using a standard stationary hot-wire instrument. The degree of the error increases with increasing intensity levels caused by the nonlinearity of the measuring system. For free shear flows such as those considered here, the local turbulence intensity is lowest at the centerline and increases radially. For the swirling jet, data is taken from Ribeiro and Whitelaw (1980). Far from the jet exit, at six diameters downstream where the flow is beginning to become fully developed, the local turbulence level near the centerline is about 20% and increases to well over 60% near the free stream. This suggests that the data from this experiment is questionable, because a stationary hot-wire was used, and no corrections were made. Consequently, we will not make quantitative comparisons between measurements and predictions.

Results for the kinetic energy and shear stress for the fully developed axisymmetric jet are shown in Figure 1. It is seen that the standard ARSM considerably over predicts the kinetic energy and shear stress compared to solutions with the RSM. These results are similar to those of Fu et al. (1988) who illustrated the

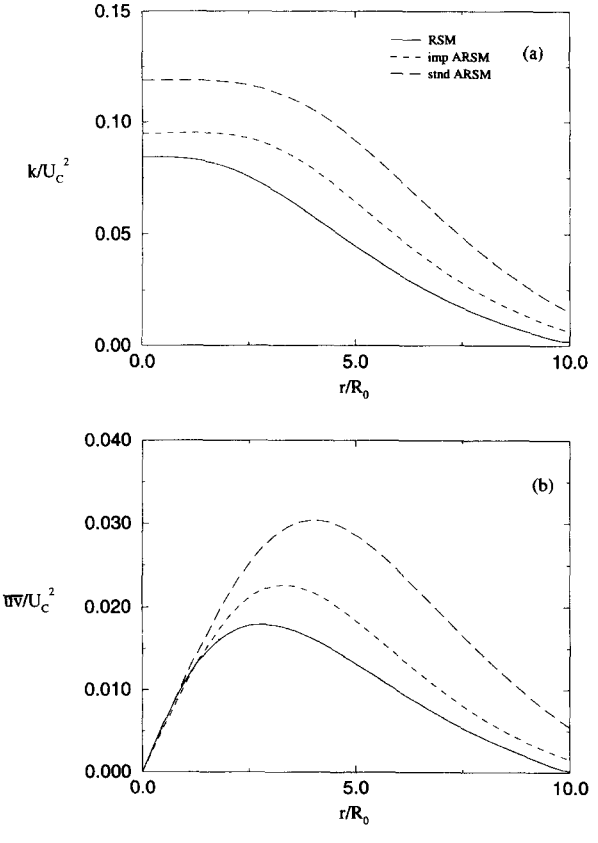

Figure 1

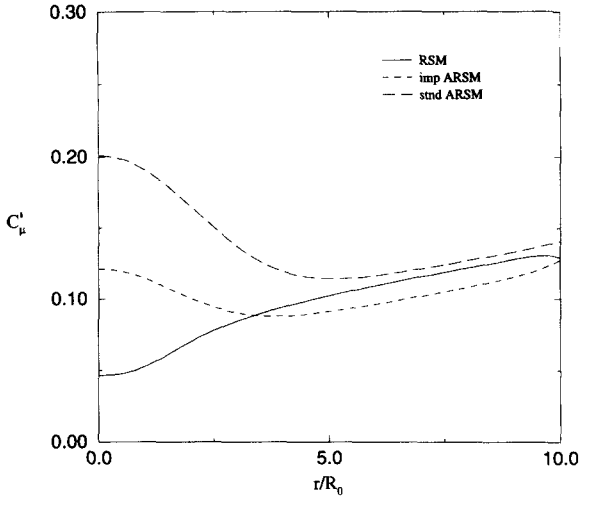

Figure 2

inadequacy of the standard ARSM for axisymmetric flows. Predictions with the improved ARSM are much closer to those obtained with the RSM. The reason for the improvement can be seen by examining the values of C'_μ as shown in Figure 2. In the case of a simple flow such as the axisymmetric jet without swirl, a total eddy viscosity coefficient can be defined so that $\overline{uv} = -C'_\mu(k^2/\epsilon)\partial U/\partial r$. For this flow, C'_μ obtained from Equation 6 is as follows:

$$C'_\mu = -\frac{1}{2}\left[G^{(1)}g + G^{(2)}\left(\frac{\partial U}{\partial x} - \frac{\partial V}{\partial r}\right)g^2\tau + G^{(3)}\left(\frac{\partial U}{\partial x} + \frac{\partial V}{\partial r}\right)g^2\tau + G^{(5)}\left[\left(\frac{\partial U}{\partial x}\right)^2 + \left(\frac{\partial V}{\partial r}\right)^2\right]g^3\tau^2 - G^{(6)}g^3\tau^2\omega^2 + G^{(7)}\left(\frac{\partial U}{\partial x} - \frac{\partial V}{\partial r}\right)g^4\tau^3\omega^2 - G^{(9)}\left(2\frac{\partial U}{\partial x} + \frac{\partial V}{\partial r}\right)g^4\tau^3\omega^2\right] \quad (15)$$

where $\omega^2 = [(\partial U/\partial r)/2]^2$. The parameter C'_μ was calculated with Equation 15 for the ARSM solutions and from $C'_\mu = -\overline{uv}/[(k^2/\epsilon)\partial U/\partial r]$ for the RSM solution. For the standard ARSM, it is seen that the C'_μ profile in Figure 2 is much too

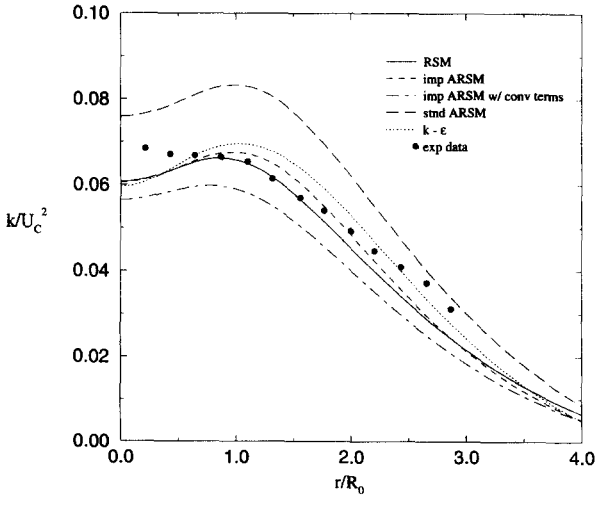

Figure 3

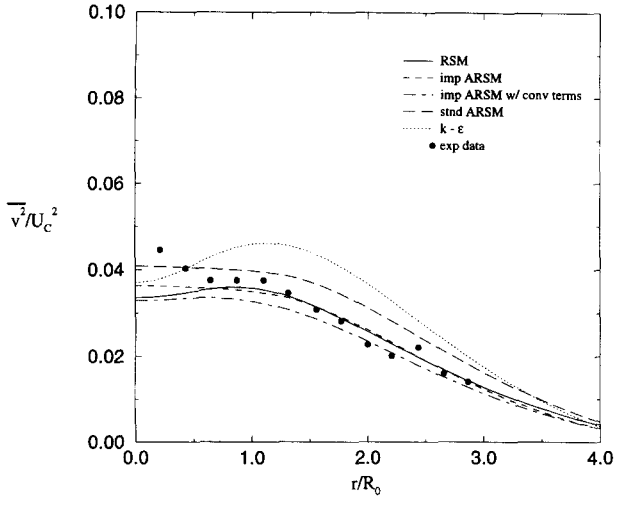

Figure 4

large near the centerline. The difference in the C'_μ profiles is attributable to the difference in the factor g appearing in the standard and improved ARSMs, as given by Equations 2 and 3.

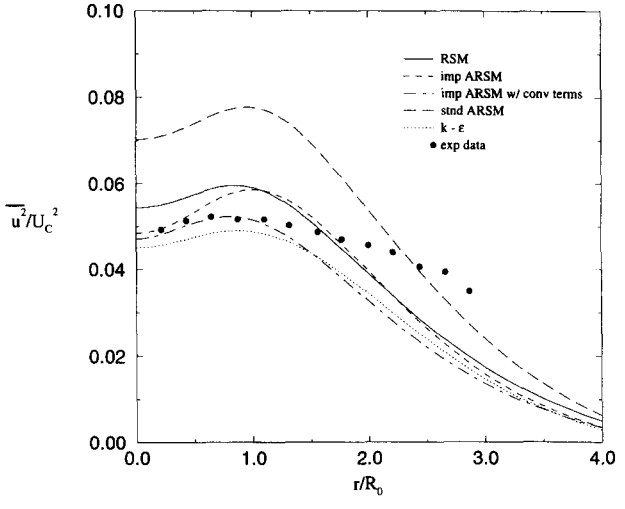

Figure 5

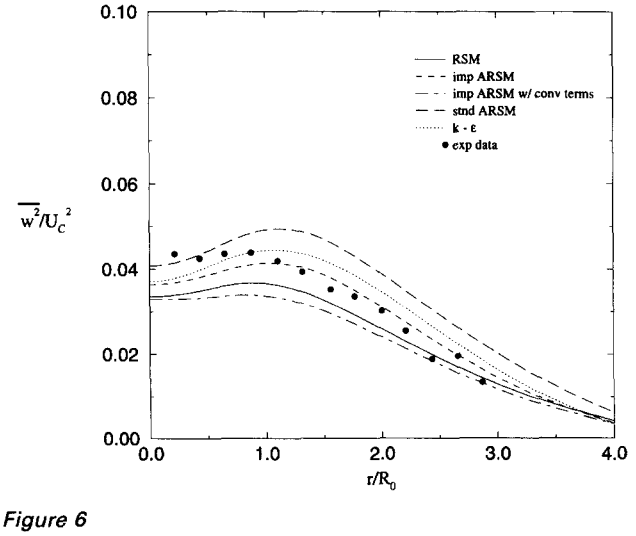

Figure 6

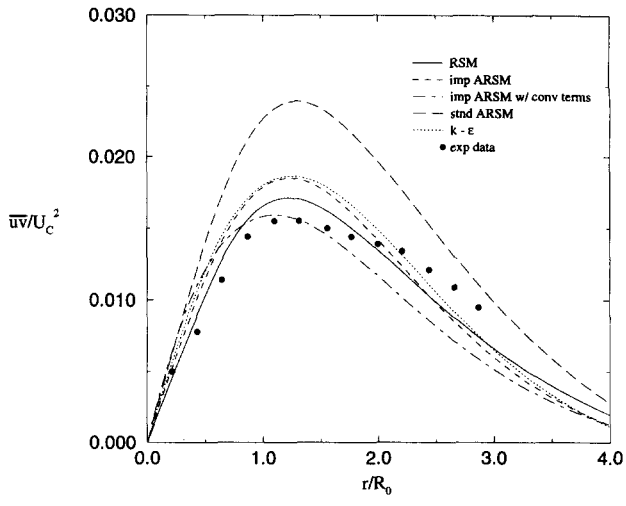

Figure 7

Approximately $C_\mu \sim 4g/15$, which gives $C_\mu \sim 0.33$ for the standard ARSM and $C_\mu \sim 0.155$ for the improved ARSM near the centerline. The improved ARSM gives a better representation of the stresses for small values of a time-scales parameter $\tau\sigma$ where $\tau = k/\epsilon$ and $\sigma = (S_{kl}S_{lk})^{1/2}$. Near the centerline of the jet, σ is small, thus, the improved ARSM gives better results there.

Calculations were also carried out for the axisymmetric swirling jet with initial conditions taken from the experimental data of Ribeiro and Whitelaw (1980) for weak swirl. Predicted results along with experimental data at six diameters ($x/D = 6.0$) from the jet exit are shown in Figures 3–8. As seen previously for the nonswirling jet and from Fu et al. (1988) for the swirling

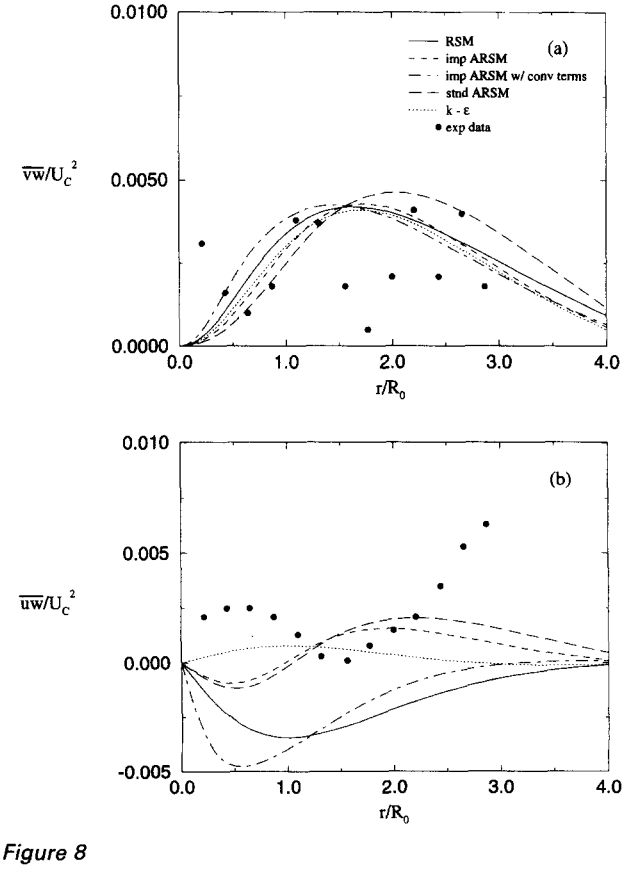

Figure 8

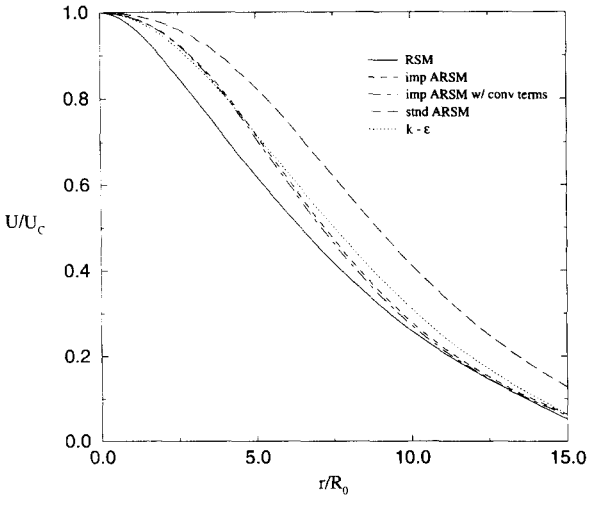

Figure 9

jet, predictions with the standard ARSM are deficient compared to results from the RSM. Results with the improved ARSM are much closer to those with the RSM. The improved ARSM with the extra convection terms from Equation 5 is somewhat better at capturing the behavior of the stresses, particularly the $\overline{uw}$ shear stress. The $k-\epsilon$ model is adequate in predicting the kinetic energy, but not the individual normal stresses; and the shear stresses, but not the $\overline{uw}$ component. There is in general adequate agreement with the experimental data from all models except the standard ARSM.

The near field ($x/D \leq 6.0$) of the swirling jet is mainly influenced by the relatively large strain field. For large axial distances, diffusional transport becomes more important. Figures 9 and 10 give profiles for the mean velocity, the kinetic energy, and the $\overline{uv}$ shear stress component at $x/D = 30.0$. It is seen that the $k-\epsilon$ and all the ARSM model predictions differ significantly from the RSM predictions, illustrating the importance of the accumulated convection and diffusion effects on the individual Reynolds stress components. It is also seen in Figures 9 and 10 that the predictions with the standard ARSM are in much less agreement with the RSM predictions than the other models. This difference is mainly a result of the poor performance of the standard ARSM in the upstream region of the flow.

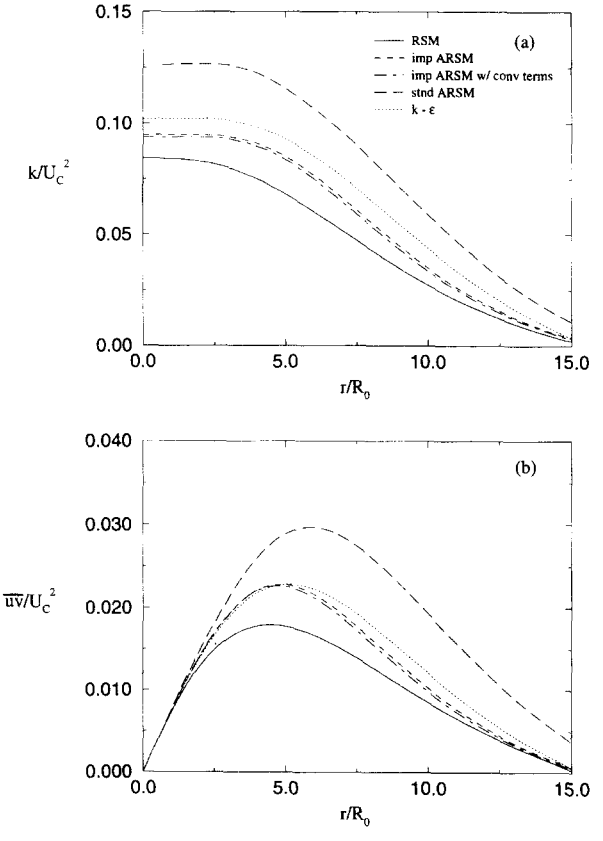

Figure 10

Summary and conclusions

The numerical solution of the modeled equations for the swirling jet demonstrates that the explicit form of the ARSM/NLSM alleviates the numerical difficulties usually associated with the implicit ARSM equation set. In the near-jet flow field predictions with the standard ARSM are considerably different than the RSM predictions. The improved ARSM, which better accounts for the range of time-scale parameter (turbulent time scale/mean flow time scale) values, gives predictions which are in reasonable agreement with those from the RSM for the near-jet field. In general, the improved ARSM gives much better predictions for the Reynolds stresses, particularly the normal components, than the $k-\epsilon$ model. Inclusion of the convection terms, which arise in the coordinate transformation, in the ARSM has a significant effect on the results for some of the shear stress components. Over relatively long flow distances, such as in the far-jet field, the convection/diffusion effects on the individual stress components become significant, and the key assumption in the ARSM formulation breaks down.

From the results obtained for the swirling jet we infer that for flows influenced by relatively large strains, the explicit NLSM obtained from the improved ARSM provides a relatively simple means of obtaining results with nearly the same quality as predicted with the RSM. The formulations involved in the NLSM lend themselves to easy implementation into existing $k-\epsilon$ computer codes. Computation times for the NLSM were only slightly greater; whereas, the RSM required several times more time as compared to the $k-\epsilon$ model.

Acknowledgments

The authors would like to acknowledge the help and contributions of J. R. Sonnenmeier to the development of the NLSM.

Appendix A

The RSM equations for the axisymmetric swirling jet come from Launder and Morse (1979):

$$\frac{\partial(\overline{u^2}U)}{\partial x}+\frac{1}{r}\frac{\partial(r\overline{u^2}V)}{\partial r}$$
$$=\frac{C_s}{r}\frac{\partial}{\partial r}\left[r\frac{k}{\epsilon}\overline{v^2}\frac{\partial\overline{u^2}}{\partial r}\right]$$
$$-2C_3\left(\overline{uv}S_{rx}+\overline{uw}S_{\theta x}+\overline{u^2}S_{xx}+\frac{1}{3}P\right)$$
$$+2C_4\left(\overline{uv}\Omega_{rx}+\overline{uw}\Omega_{\theta x}\right)+\frac{2}{3}\left(C_1-1+\frac{P}{\epsilon}\right)\epsilon-\gamma kS_{xx}$$
$$-C_1\frac{\epsilon}{k}\overline{u^2}$$

$$\frac{\partial(\overline{v^2}U)}{\partial x}+\frac{1}{r}\frac{\partial(r\overline{v^2}V)}{\partial r}-2W\frac{\overline{vw}}{r}$$
$$=\frac{C_s}{r}\frac{\partial}{\partial r}\left[r\frac{k}{\epsilon}\left(\overline{v^2}\frac{\partial\overline{v^2}}{\partial r}-2\frac{(\overline{vw})^2}{r}\right)\right]$$
$$-2\frac{C_s}{r}\frac{k}{\epsilon}\left[\overline{vw}\frac{\partial\overline{vw}}{\partial r}+\overline{w^2}\left(\frac{\overline{v^2}-\overline{w^2}}{r}\right)\right]$$
$$-2C_3\left(\overline{v^2}S_{rr}+\overline{vw}S_r\theta+\overline{uv}S_{rx}+\frac{1}{3}P\right)$$
$$-2C_4\left(\overline{vw}\Omega_{r\theta}+\overline{uv}\Omega_{rx}\right)+\frac{2}{3}\left(C_1-1+\frac{P}{\epsilon}\right)\epsilon-\gamma kS_{rr}$$
$$-C_1\frac{\epsilon}{k}\overline{v^2}$$

$$\frac{\partial(\overline{w^2}U)}{\partial x}+\frac{1}{r}\frac{\partial(r\overline{w^2}V)}{\partial r}+2W\frac{\overline{vw}}{r}$$
$$=\frac{C_s}{r}\frac{\partial}{\partial r}\left[r\frac{k}{\epsilon}\left(\overline{v^2}\frac{\partial\overline{w^2}}{\partial r}+2\frac{(\overline{vw})^2}{r}\right)\right]$$
$$+2\frac{C_s}{r}\frac{k}{\epsilon}\left[\overline{vw}\frac{\partial\overline{vw}}{\partial r}+\overline{w^2}\left(\frac{\overline{v^2}-\overline{w^2}}{r}\right)\right]$$
$$-2C_3\left(\overline{w^2}S_{\theta\theta}+\overline{vw}S_{r\theta}+\overline{uw}S_{\theta x}+\frac{1}{3}P\right)$$
$$+2C_4\left(\overline{vw}\Omega_{r\theta}-\overline{uw}\Omega_{\theta x}\right)+\frac{2}{3}\left(C_1-1+\frac{P}{\epsilon}\right)\epsilon-\gamma kS_{\theta\theta}$$
$$-C_1\frac{\epsilon}{k}\overline{w^2}$$

$$\frac{\partial(\overline{uv}U)}{\partial x}+\frac{1}{r}\frac{\partial(r\overline{uv}V)}{\partial r}-W\frac{\overline{uw}}{r}$$
$$=\frac{C_s}{r}\frac{\partial}{\partial r}\left[r\frac{k}{\epsilon}\left(\overline{v^2}\frac{\partial\overline{uv}}{\partial r}-\frac{\overline{vwuw}}{r}\right)\right]-\frac{C_s}{r}\frac{k}{\epsilon}\left[\overline{vw}\frac{\partial\overline{uw}}{\partial r}+\overline{w^2}\frac{\overline{uv}}{r}\right]$$
$$-C_3\left[\left(\overline{v^2}+\overline{u^2}\right)S_{rx}+\overline{vw}S_{\theta x}+\overline{uv}(S_{rr}+S_{xx})+\overline{uw}S_{r\theta}\right]$$
$$+C_4\left[\left(\overline{v^2}-\overline{u^2}\right)\Omega_{rx}+\overline{vw}\Omega_{\theta x}-\overline{uw}\Omega_{r\theta}\right]-\gamma kS_{rx}-C_1\frac{\epsilon}{k}\overline{uv}$$

$$\frac{\partial(\overline{vw}U)}{\partial x}+\frac{1}{r}\frac{\partial(r\overline{vw}V)}{\partial r}+W\left(\frac{\overline{v^2}-\overline{w^2}}{r}\right)$$
$$=\frac{C_s}{r}\frac{\partial}{\partial r}\left\{r\frac{k}{\epsilon}\left[\overline{v^2}\frac{\partial\overline{vw}}{\partial r}+\overline{vw}\left(\frac{\overline{v^2}-\overline{w^2}}{r}\right)\right]\right\}$$
$$+\frac{C_s}{k}\frac{k}{\epsilon}\left[\overline{vw}\frac{\partial}{\partial r}\left(\overline{v^2}-\overline{w^2}\right)-4\overline{w^2}\frac{\overline{vw}}{r}\right]$$
$$-C_3\left[\left(\overline{v^2}+\overline{w^2}\right)S_{r\theta}+\overline{uv}S_{\theta x}+\overline{vw}(S_{rr}+S_{\theta\theta})+\overline{uw}S_{rx}\right]$$
$$+C_4\left[\overline{v^2}\Omega_{r\theta}-\overline{uv}\Omega_{\theta x}-\overline{w^2}\Omega_{r\theta}-\overline{uw}_{rx}\right]-\gamma kS_{r\theta}-C_1\frac{\epsilon}{k}\overline{vw}$$

$$\frac{\partial(\overline{uw}U)}{\partial x}+\frac{1}{r}\frac{\partial(r\overline{uw}V)}{\partial r}+W\frac{\overline{uv}}{r}$$
$$=\frac{C_s}{r}\frac{\partial}{\partial r}\left[r\frac{k}{\epsilon}\left(\overline{v^2}\frac{\partial\overline{uw}}{\partial r}+\overline{vwuv}\right)\right]+\frac{C_s}{r}\frac{k}{\epsilon}\left[\overline{vw}\frac{\partial\overline{uv}}{\partial r}-\overline{w^2}\frac{\overline{uw}}{r}\right]$$
$$-C_3\left[\left(\overline{w^2}+\overline{u^2}\right)S_{\theta x}+\overline{vw}S_{rx}+\overline{uw}(S_{\theta\theta}+S_{xx})+\overline{uv}S_{r\theta}\right]$$
$$+C_4\left[\left(\overline{w^2}-\overline{u^2}\right)\Omega_{\theta x}+\overline{vw}\Omega_{rx}+\overline{uv}\Omega_{r\theta}\right]-\gamma kS_{\theta x}$$
$$-C_1\frac{\epsilon}{k}\overline{uw}$$

Appendix B

$$S_{xx}=\frac{\partial U}{\omega x}$$
$$S_{rr}=\frac{\partial V}{\partial r}$$
$$S_{\theta\theta}=\frac{V}{r}$$
$$S_{rx}=\frac{1}{2}\frac{\partial U}{\partial r}$$
$$S_{r\theta}=\frac{1}{2}\left[\frac{\partial W}{\partial r}-\frac{W}{r}\right]$$
$$S_{\theta x}=\frac{1}{2}\frac{\partial W}{\partial x}=0$$
$$\Omega_{rx}=-\Omega_{xr}=-\frac{1}{2}\frac{\partial U}{\partial r}$$
$$\Omega_{r\theta}=-\Omega_{\theta r}=-\frac{1}{2}\left[\frac{\partial W}{\partial r}+\frac{W}{r}\right]$$
$$\Omega_{\theta x}=-\Omega_{x\theta}=\frac{1}{2}\frac{\partial W}{\partial x}=0$$

Appendix C

$$\Omega^*_{rx}=-\Omega^*_{xr}=-g\tau\frac{1}{2}\frac{\partial U}{\partial r}$$
$$\Omega^*_{r\theta}=-\Omega^*_{\theta r}=-g\tau\left[\frac{1}{2}\left(\frac{\partial W}{\partial r}+\frac{W}{r}\right)+\frac{W}{r}\frac{1}{C_4}\right]$$
$$\Omega^*_{\theta x}=-\Omega^*_{x\theta}=g\tau\frac{1}{2}\frac{\partial W}{\partial x}=0$$

References

Ekander, H. and Johansson, A. V. 1989. An improved algebraic Reynolds stress model and application to curved and rotating channel flows. *Proc. 7th Symposium on Turbulent Shear Flows*, 21.2.1–21.2.6

Fu, S., Huang, P. G., Launder, B. E. and Leschziner, M. A. 1988. A comparison of algebraic and differential second-moment closures for axisymmetric turbulent shear flows with and without swirl. *J. Fluids Eng.*, **110** 216–221

Gibson, M. M. and Younis, B. A. 1986. Calculation of swirling jets with a Reynolds stress closure. *Phys. Fluids*, **29**, 38–48

Hogg, S. and Leschziner, M. A. 1989. Computation of highly swirling confined flow with a Reynolds stress turbulence model. *AIAA J.* **27**, 57–63

Hussein, H. J., Capp, S. P. and George, W. K. 1994. Velocity measurements in a high Reynolds number, momentum-conserving, axisymmetric, turbulent jet. *J. Fluid Mech.*, **258**, 31–75

Jones, W. P. and Pascau, A. 1989. Calculation of confined swirling flows with a second moment closure. *J. Fluids Eng.*, **111**, 248–255

Kim, K. Y. and Chung, M. K. 1988. Calculation of a strongly swirling turbulent round jet with recirculation by an algebraic stress model. *Int. J. Heat Fluid Flow*, **9**, 62–68

Launder, B. E. 1971. Imperial College Mechanical Engineering Report TM/TN/A/9

Launder, B. E., Reece, G. and Rodi, W. 1975. Progress in the development of a Reynolds-stress turbulence closure. *J. Fluid Mech.*, **68**, 537

Launder, B. E. and Morse, A. 1979. Numerical prediction of axisymmetric free shear flows with a second-order Reynolds-stress closure. *Turbulent Shear Flows*, **1**, 4.21–4.30

Leschziner, M. A. and Rodi, W. 1984. Computation of strongly swirling axisymmetric free jets. *AIAA J.* **22**, 1742–1747

Naji, H. 1986. The prediction of turbulent swirling jet flow. *Int. J. Heat Mass Transfer*, **29** 169–182

Ribeiro, M. M. and Whitelaw, J. H. 1980. Coaxial jets with and without swirl. *J. Fluid Mech.*, **96**, 769–795

Rodi, W. 1972. The prediction of free turbulent boundary layers by use of a two equation model of turbulence. Ph.D. thesis, University of London, London, UK

Rodi, W. 1976. A new algebraic stress relation for calculating the Reynolds stresses. *Z. Angew. Math. Mech.*, **56**, 219

Taulbee, D. B. 1989. Engineering turbulence models. In *Advances in Turbulence*. Hemisphere Bristol, PA 75–125

Taulbee, D. B. 1992. An improved algebraic Reynolds stress model and corresponding nonlinear stress model. *Phys. Fluids A*, **4**, 2555–2561

Taulbee, D. B., Sonnenmeier, J. R. and Wall, K. M. 1994. Stress relation for three dimensional turbulent flows. *Phys. Fluids*, **6**, 1399–1401